Soils and Rocks
An International Journal of Geotechnical and Geoenvironmental Engineering
www.soilsandrocks.com
ISSN 1980-9743
ISSN-e 2675-5475

Design, construction, and validation of an experimental inclinometer probe

Tennison Freire de Souza Junior[1#], José Lucas Silva Borges[1], Cezar Falavigna Silva[2], Karla Salvagni Heineck[1]

Article

Keywords
Low cost
Geotechnical instrument
Inclinometer
Monitoring
Experimental probe
Horizontal displacement

Abstract

The inclinometer probe is used to measure angle variations along a soil profile. These variations can be transformed into horizontal displacements along the profile depth, enabling the understanding of the deformation of geotechnical structures (e.g., tailings dams, embankment dams, rockfill dams, and excavations) and natural slopes. Such knowledge can guide preventive and corrective actions and mitigation measures to reduce the severity of socioeconomic and environmental impacts. In this study, a low-cost, reduced-dimension inclinometer probe was developed and validated. Accessible technologies (MEMS inclinometer sensor, microprocessor, logic level converters, communication module, and other electronic components) were used for the probe. The sensor reading programming was developed using Python language and interpreted using an Excel spreadsheet. The probe was calibrated on a three-dimensional measurement table with the aid of a mechanical device to stabilize its inclination and validated by comparison of its output with those of a commercial probe. The probe had a lower cost than commercial probes and generated similar readings, although the reading time was longer due to the increased number of measurements required.

1. Introduction

The inclinometer, also known as the inclinometric probe, is a well-established instrument for measuring soil behavior in the field of geotechnics. This instrument is designed to monitor the rates of horizontal displacement of geotechnical structures (slopes, embankments, dams, etc.) over time and soil depth (Silveira, 2006; Bo & Barrett, 2023). The inclinometer was developed based on a device built in 1952 by S.D. Wilson of Harvard University and was made commercially available by the end of the 1950s by the Slope Indicator Company (Green & Mikkelsen, 1988).

Penz (2013) indicated that the term "inclinometer" refers to "every instrument that due to the constructive characteristics propitiates the measurement of the local inclination or to verify the existence of angular variations, being the process done in a differential or absolute manner.". Most aspects of these instruments are described in the geotechnical literature (e.g., Dunnicliff, 1988; Green & Mikkelsen, 1988; Mikkelsen, 2002, 2003; Silveira, 2006; Stark & Choi, 2008; Fernandes, 2011). Coimbra et al. (2023) conducted a review of the state of the art and practice regarding the operation of inclinometers for slope monitoring in geotechnical works.

Dunnicliff (1988) and Stark & Choi (2008) reported that inclinometers are used to determine the magnitude, rate, direction, depth, and type of soil movement. Generally, this information is vital for the understanding of landslide causes, behavior, and correction requirements, although this objective cannot be achieved without continuous monitoring. Hunt (2005) noted that the continuous measurement of lateral deflection from the surface with an inclinometer is very useful in the monitoring of embankments and pile foundations.

Over time, the inclinometer has been refined and has become more accurate (e.g., Wilson, 1962; Hanna, 1985; Silveira, 2006; Machan & Bennett, 2008). In the literature, there are experimentally developed inclinometric probes (e.g., Formoso, 1999; Penz, 2013; Covassi et al., 2018). From a commercial point of view, the technological development of these devices occurred with the advent of the 21st century and the introduction of MEMS accelerometers and wireless (i.e., via Bluetooth and Wi-Fi) data transfer. Freddi et al. (2023) introduced an automated in-place inclinometer system using MEM sensors. Manufacturers such as the Slope Indicator Company, Geokon, Geodaq, and Encardiorite have developed more versatile, efficient, and accurate probes. The in-place ShapeArray inclinometer developed by Measurand is used

[#] Corresponding author. E-mail address: tennisongeotec@gmail.com
[1] Universidade Federal do Rio Grande do Sul, Departamento de Engenharia Civil, Porto Alegre, RS, Brasil.
[2] Universidade Federal do Paraná, Departamento de Construção Civil, Curitiba, PR, Brasil.

Submitted on June 19, 2023; Final Acceptance on April 12, 2024; Discussion open until February 28, 2025.
https://doi.org/10.28927/SR.2024.000623

in the instrumentation of dams, embankments, slopes, and excavations.

Despite its importance, the monitoring of small and medium geotechnical constructions and natural slopes on highways and in urban areas is incipient because the significant costs of guide tube installation, probe purchase or rental, technical support, monitoring, and maintenance make it financially unfeasible. In this work, we developed and validated a reduced-proportion, low-cost inclinometer probe to aid the dissemination of inclinometer use at geotechnical sites and on natural slopes.

2. Background

2.1 Reading procedures and data interpretation

Stark & Choi (2008) and Dunnicliff (1988) explained that inclinometers generate a zero reading or initial profile, established with at least two readings, that serves as a reference. Dunnicliff (1988) noted that in case of doubt, the absolute transverse deformation of the top of the guide tube should be monitored regularly using topographic survey methods. Slope measurements should be acquired starting from the inclinometer's stable base (Dunnicliff, 1988; Stark & Choi, 2008). In the reading procedure in conventional inclinometers, the probe is lowered slowly to the desired depth using the intervals in the cable (0.5−1 m). Before the zero readings are taken, the probe must be held in position for at least 10 min to adjust to the temperature in the hole. Dunnicliff (1988) listed the subsequent procedures:

- the taking of readings at different depths;
- the removal of the probe, its rotation through 180°, and its lowering again to the same point;
- the taking of readings at different depths after temperature stabilization; and
- verification of the validity of the checksums.

The 180º rotation of the probe is necessary to distribute the reading errors (e.g., sensor position and wheellock play). Stark & Choi (2008) further explained that the probe is lowered to the bottom of the guide tube with the wheels in the A0° groove for the taking of the first measurements after the zero readings. When the probe reaches the bottom of the inclinometer, the cable is attached to the pulley grips at the foot marker corresponding to the lowest depth reached for the initial readings.

The probe should then be lifted to the surface in the intended increments, with readings taken from the A0° and B0° directions at each interval (Figure 1). A measuring range equal to the probe wheelbase is commonly used to achieve maximum accuracy.

The B0° direction is 90° clockwise from A0°, and the tilt on the B axis is measured by the second sensor on the probe. After all readings have been taken with the wheels in the A0° slot and the probe hits the surface, the probe is carefully removed and rotated 180° so that the lower wheels are inserted into the A0° slot and another set of readings is taken in the A180° and B180° directions.

Souza et al. (2016) pointed out that the guide tube must have a minimum length of 5 m from its lower section fixed below the greatest depth at which some movement is expected. Thus, the end of this tube can be considered as a fixed reference. Bartholomew et al. (1987) explained that the inclinometer probe measures angles of inclination from

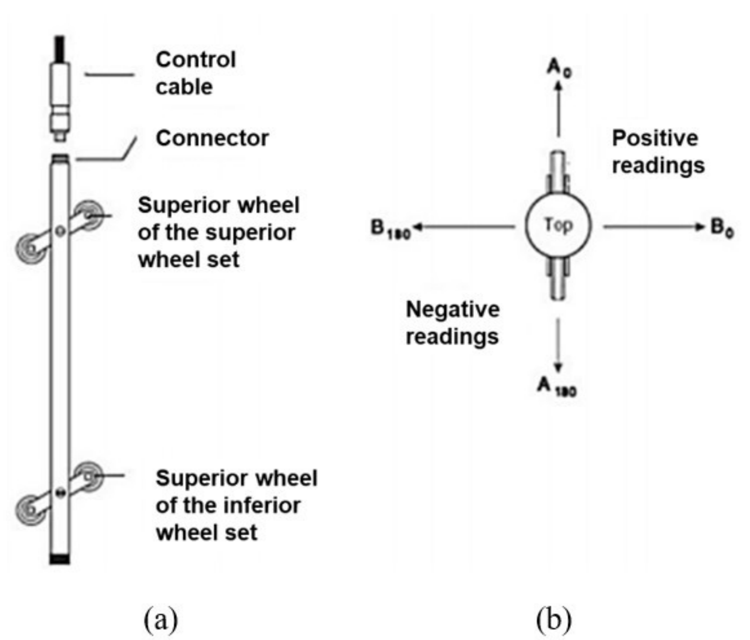

Figure 1. Schematic drawings of the inclinometer probe: (a) side view; (b) top view.

vertical in two planes oriented at 90° (orthogonally) to each other, which can be uniaxial or biaxial (Figure 2). With uniaxial probes, two additional series of measurements are taken when deformation data from both vertical planes are needed by aligning the probe wheels in the second pair of grooves (i.e., 90° relative to the first series; Dunnicliff, 1988).

Stark & Choi (2008) emphasized the importance of using the same probe (to reduce possible errors) and measuring displacements at the same depth intervals as the initial reading. The deviation from vertical displacement, that is, the horizontal displacement (Figure 2), is determined by a sinusoidal function using Equation 1:

$$\delta_{DH} = \mathrm{L} \cdot \sin\theta \tag{1}$$

Where δ_{DH} is the calculated horizontal displacement, L is the distance in pairs of probe wheels and è is the rotation angle of the probe. The vertical deviation in each measurement range reflects the lateral position of the guide tube to the fixed end. The total horizontal (cumulative) displacement is obtained by summing the individual lateral deviations between the fixed end and the top of the guide tube using Equation 2:

$$\delta_{DHT} = \sum \delta_{DH} \tag{2}$$

2.2 Sources of error

Green & Mikkelsen (1988) and Stark & Choi (2008) stated that the accuracy and reliability of measured positions and displacement profiles depend on the quality of an inclinometer's housing, probe, cable, readings, and selected accessories. The sensor quality (resolution, sensitivity, offset, accuracy, and precision) is of great relevance for the faithful representation of displacements. In addition to the quality of the equipment, the accuracy, precision, and reliability of inclinometer monitoring data depend on factors such as the installation and measurement methods, the functionality and performance of the installed instrument (Bo & Barrett, 2023).

Dunnicliff (1988) and Souza et al. (2016) noted that inclinometers' sensor wheels commonly have a certain clearance to the orthogonal direction, which results in the generation of more errors along the B axis. This clearance originates from imperfections in the grooves of the tube or from sensor wheel wear.

In the current context, the term "error" refers to random and systematic errors and is important for landslides that have not moved significantly. If the movement measured on a tilt inclinometer does not exceed the system's field accuracy, the consultant or expert should view it carefully and assess whether it is within the probe's expected error (Stark & Choi,

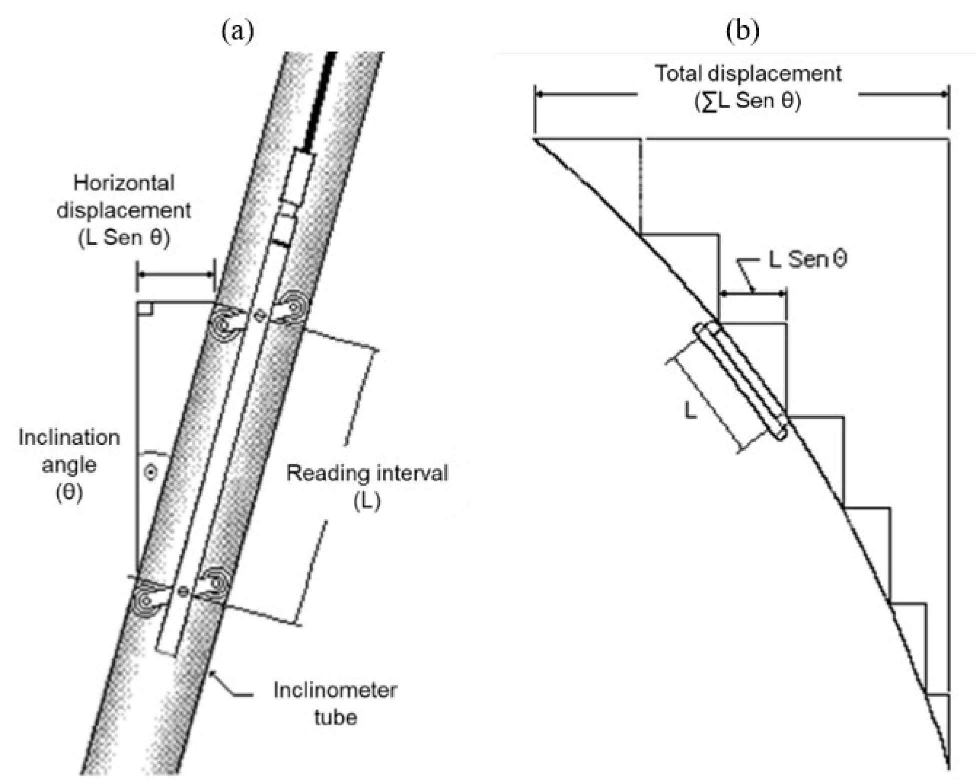

Figure 2. Schematic drawings of the reading procedure: (a) detail of the probe inserted into the tube; (b) reading along the entire length of the tube (adapted from Dunnicliff, 1988).

2008). Mikkelsen (2003) listed four systematic errors that affect inclinometer measurements:

- tilt (bias) shift;
- sensitivity deviation;
- rotation; and
- depth position errors.

3. Experimental program

The experimental program was carried out in five stages. First, the electronic components used for the construction of the internal measurement and communication circuit were selected. Next, the geometric design of the small-proportion probe was developed. Then, the probe assembly, reading, and operation procedures were described. The probe was constructed, assembled, and calibrated, and, finally, the equipment was validated by comparison with a commercially available inclinometer probe.

4. Materials

The components of the probe, including its electronic circuit, are listed in Table 1.

4.1 Electronic components and circuits

Among the MEMS accelerometers available on the electronics market, the SCA 103T D04-1 (Murata, 2019; Figure 3a) was selected for the inclinometer probe. Its parameters are listed in Table 2, This accelerometer has high calibration accuracy, high resolution, and a low noise level. It is not sensitive to vibration because its sensory elements are dampened, and it can withstand mechanical shocks of 20,000 g. This accelerometer can be used for platform leveling and stabilization, laser level rotation, instrument leveling, and level building.

The electrical connection of the accelerometer for tilt measurements is performed using pins 5 (OUT_2) and 11 (OUT_1; Aa). Ab shows typical outputs (channels 1 and 2 and differential output OUT_1–OUT_2). Rotation angles are calculated as a function of the output's electrical response (Figure 4).

Voltage measurements (analog outputs) can be converted to the accelerometer's inclination angle (α; Murata, 2019), which represents the probe body's angle of rotation, using Equation 3:

$$\mathrm{A} = \arcsin\left(\frac{V_{D,out} - Offset}{sensitivy}\right) \tag{3}$$

Inclination angles close to 0° can be estimated accurately with straight-line conversion, but the use of arcsine conversion is preferred for the greatest accuracy (Murata, 2019). The sensor sensitivity (in V/g) is calculated using Equation 4, considering the sensor position and electrical output voltage:

$$\text{Sensitivity } = \left(\frac{Vout_{tilt\,1} - Vout_{tilt\,2}}{\sin(tilt\,1) + \sin(tilt\,2)}\right). \tag{4}$$

Table 1. Experimental inclinometer probe components.

Item	Unit	Quantity
Inclinometer's probe body - stainless steel 304	Unit	1
Reading unit housing - stainless steel 316	Unit	1
Base (3D printing) - ABS	Unit	1
MEMS Accelerometer SCA 103T D04-1	Unit	2
Analog/Digital Converter Module - ADS 1115 (4 channels)	Unit	1
RS-485 module	Unit	2
Plastic case (100 mm × 60 mm × 25 mm)	Unit	1
TTL-USB Converter	Unit	1
Logic level converter module	Unit	1
Mike connector 5 pins PCI F/M 025-70	Unit	1
Key NA Push Button DS-323 without Thermal Lock 023-9	Unit	1
Raspberry Pi 0 W Anatel board	Unit	1
1/8” stainless steel cable clips	Unit	3
3/32” 2.4 mm 6×7 AA stainless steel cable	m	21
Shielded network cable - 4 pairs	m	20
Plastic spool	Unit	1
Centering CAP (75 mm / 86 mm)	Unit	1
Nylon cable ties 100 mm × 2.5 mm	Pkt	1
Cable gland	Unit	1
O-ring	Unit	1

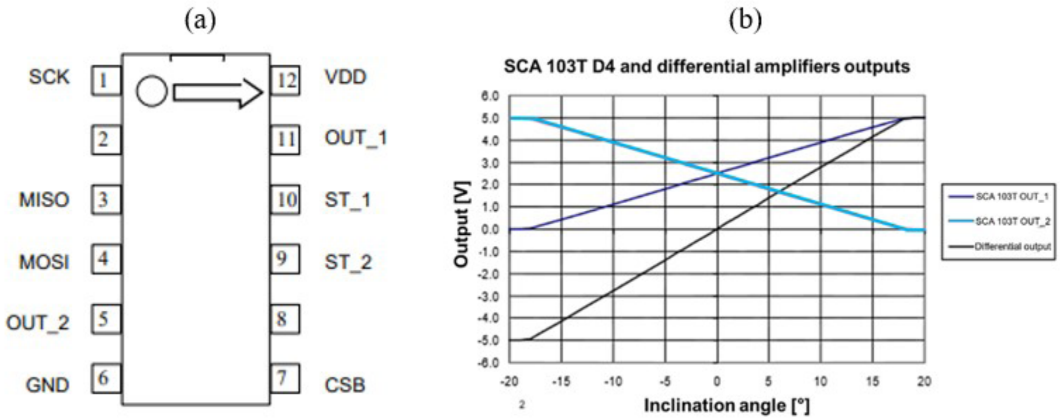

Figure 3. Electrical connection of the SCA 103T D04-1 MEMS accelerometer: (a) circuit diagram; (b) output behavior (adapted from Murata, 2019).

Table 2. SCA 103T D04-1 MEMS accelerometer parameters (adapted from Murata, 2019).

Parameter	Unit	Values
Measurement range	°	± 15
Force	g	± 0.26
Gravitational analog sensitivity	V/g	16
Angular analog sensitivity	mV/°	280
Digital resolution	°/LSB	0.009
Analog resolution	°	0.0013
Operating temperature	°C	-40 – 125
Typical non-linearity	°	± 0.057
Typical consumption current	mA	4 (5*)
Supply voltage Vdd	V	4.75 – 5.25 (5**)

*The maximum consumption current is 5 mA. **The typical supply voltage is 5 V.

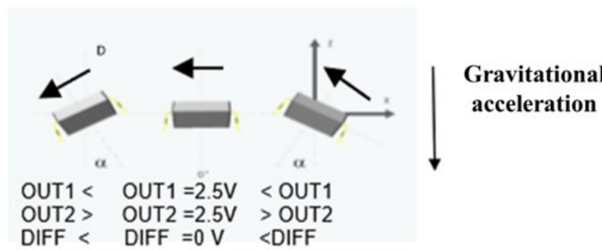

Figure 4. Behavior of the SCA 103T D04-1 analog output (adapted from Murata, 2019).

A Raspberry Pi Zero single-board computer (65 × 30 × 5 mm), made of low-cost components (Adafruit, 2019), was used for data acquisition (Figure 5a). The body of the computer's board is made up of a 1 GHz single-core ARM processor (CPU; similar to the B+ and A+ Pi models) and 512 MB RAM memory unit. The board has a mini-HDMI port (with PAL or NTSC output through two 0.1" pads), micro-USB OTG port, micro-USB power port, and HAT-compatible 40-pin header. Figure 5b shows an illustration of the MEMs sensor, model SCA 103T D04-1 and manufactured by Murata . Technical data is given in Table 2.

A low-cost module based on MAX485ESA chip (Maxim), capable of establishing differential communication according to the RS-485 standard was used (Figure 5c). The operating voltage used was 3.3 V, the same as applied to all other devices. This module's power consumption is 300 µA (Maxim, 2014) and the long-distance communication was established through a shielded network cable according to the Cat5e standard (Figure 5g).

The conductors are four pairs of intertwined copper wires with individual thermoplastic protection. A USB-TTL module (Figure 5d) was used to convert the communication standards used for the microcontrollers (UART or TTL) to USB ports communication pattern (RS-232). This module uses a PL-2303 chip (Prolific), which requires a 24 mA current for operation. To adjust the voltage supplied by the USB port to the input level requested by the devices (5 V), the XL6009E1 (XLSEMI) voltage regulator was used (Figure 5e).

This type of regulator was selected because it has more operational efficiency than other devices. Its operation requires a 5-mA current. In an adjustment of the initial plan, the ADS-1115 (Texas Instruments) analog/digital converter (Figure 5f), which has a 16-bit resolution, was applied to the analog sensor output.

The total cost for the electronic components and machining of the metal parts for the inclinometer probe was 10–20% of that of a commercially available inclinometer probe.

The internal circuit of the inclinometer can be visualized through Figure 6a. The system is powered and the data are viewed via the computer's USB port. To overcome voltage drop along the cable and ensure that a voltage of 5V is maintained, a step-up voltage regulator (Figure 6b) was used. A logic level converter was applied to the communication between the sensor and the Raspberry Pi Zero, as their operating voltages are 5 and 3.3 V, respectively. Two RS-485 modules were used to create a standard signal emission that enables long-

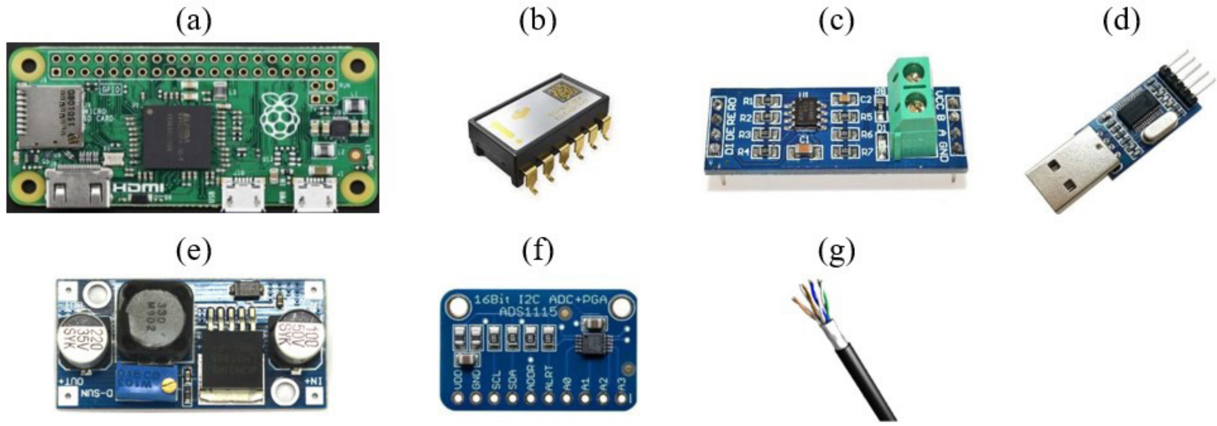

Figure 5. Inclinometer electronic components: (a) Raspberry Pi Zero W board; (b) MEMS SCA 103T D04-1 sensor; (c) RS-485 module; (d) USB-TTL module; (e) voltage regulator; (f) ADS-1115 module; (g) communication cable.

distance communication between the probe and the notebook through a TTL-USB converter (Figure 6c). The USB input enables communication between the inclinometer and the notebook and is the power source for the probe's electronic components.

4.2 Inclinometer probe body

The probe design, including conceptual details of the longitudinal sections, is presented as Figure 6. The distance between wheel axes was 15 cm, based on Penz (2013). This reduced distance provides for a more precise description of localized displacements and ease of removal of the equipment inside the guide tube. The design specifications and geometric dimensions of the inclinometer, in cut sections, are shown in Figure 7 and Figure 8, respectively.

The larger section in the upper region of the case accommodates the 35-mm-wide Raspberry Pi Zero W board. The probe body is made of grades 304 and 316 (in the chamber) stainless steel. Stainless steel is alloyed with iron, carbon, and a minimum of 10.50% chromium (Cr), which guarantees corrosion resistance (Carbó, 2008). Grade 304 stainless steel contains nickel (Ni) as an alloying element, which changes the ferritic structure to austenitic. More specifically, this steel has 18% Cr and 8% Ni contents and is the most popular grade due to its excellent corrosion resistance, ductility (a marked difference in mechanical properties from ferritic steel), and weldability. However, it can be corroded by the chloride anion (Cl^-). Depending on the concentration of chlorides in the exposure medium, and the temperature and pH, three forms of corrosion can occur: pitting, crevice development, and/or stress.

According to ASTM A479 (ASTM, 2007), 316 stainless steel is composed of an alloy that includes chromium, nickel, and molybdenum. The introduction of molybdenum (the 304 stainless is free) gives the material greater chemical resistance in highly corrosive environments, such as salt water or chlorides. In addition, it has a better resistance to creep at higher temperatures and a higher mechanical resistance compared to stainless 304.

Finally, grades 304 and 316 stainless steel are austenitic and thus not magnetic, and thus are suitable for electronic equipment. Figure 9 shows the machined and welded probe body with the introduction of the cable gland for the data cable output.

5. Probe function

The electronic circuit initially works via the MEM sensors, which measure the inclination continuously based on gravitational acceleration and transform this information into output data (Figure 4). These data are converted to digital readings and sent via SPI communication to the Raspberry Pi Zero board, and then via the serial port to the RS-485 module. Another RS-485 module and a TTL-USB converter receive the data sent via cable and provide them to the computer. All these tasks were programmed using the Python language.

To perform measurements and obtain a displacement graph, the following sequence of procedures must be followed:

1) Open the inclinometer.py routine file;
2) Inform the COM port activated by the USB port through the reading cable on the inclinometer probe and press the "enter" key (Figure 10);
3) Inform the serial value in the program (9600) and press the "enter" key (Figure 10);
4) Position the inclinometer at the reading depth;
5) Press the "y" button in response to the question "Do you want to collect a reading? [y,n]; once the probe has stabilized for the last 50 readings, the digital reading value is reported (Figure 10);
6) Reposition the equipment to the next measurement depth and repeat the entire procedure;

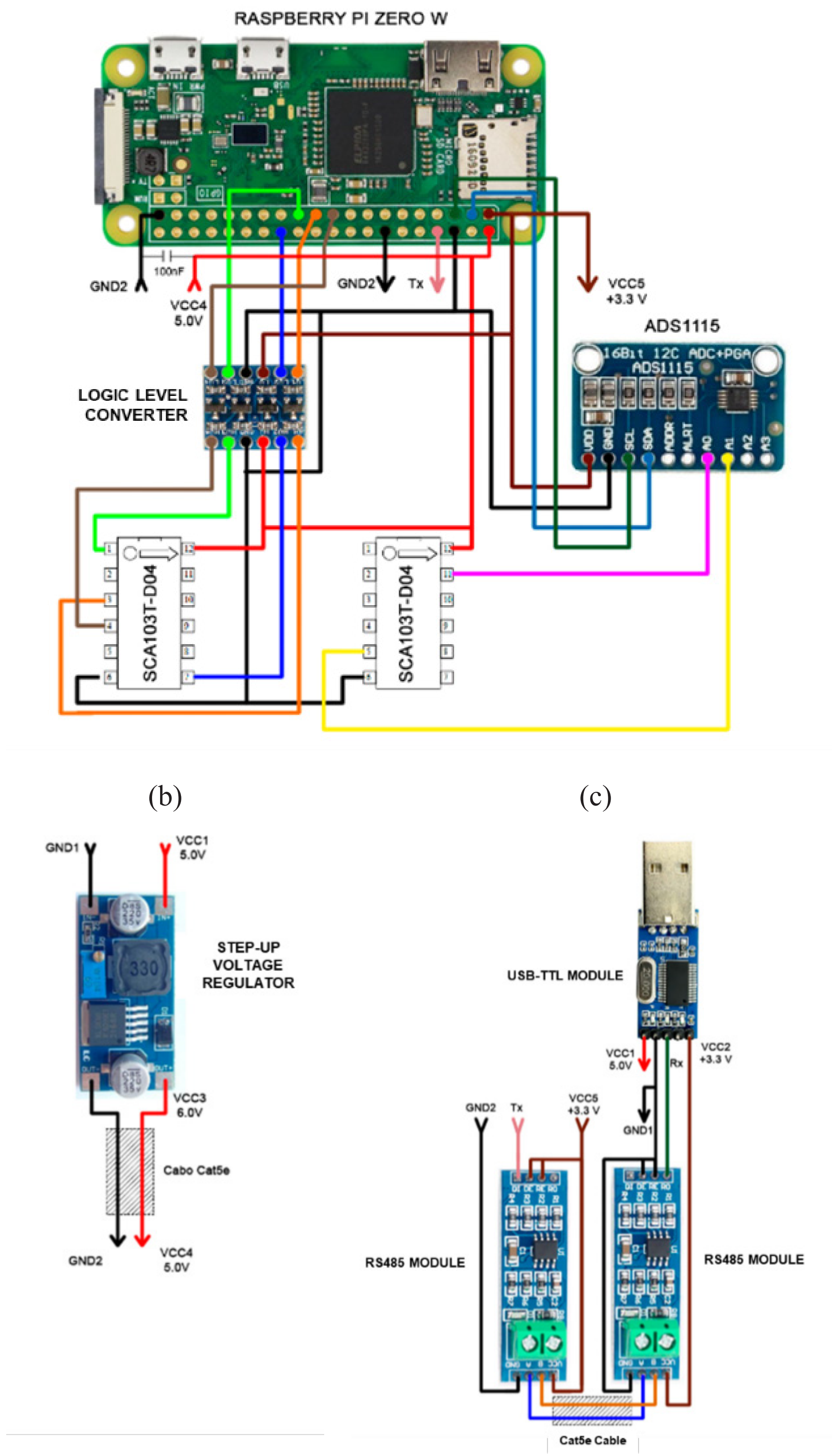

Figure 6. Electrical circuits of the inclinometer: (a) main circuit; (b) step-up voltage regulator; (c) secondary circuit to connect the main circuit to a notebook.

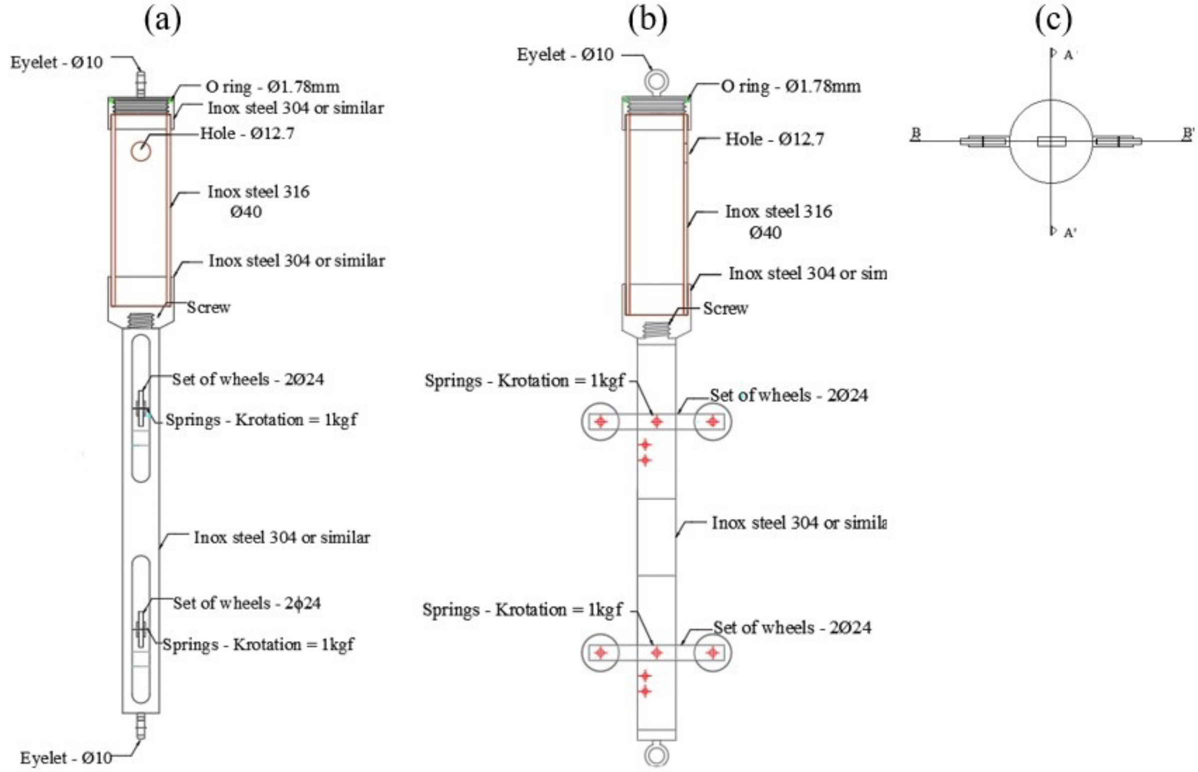

Figure 7. Conceptual drawings of the inclinometer probe: (a) A–A' section; (b) B–B' section; (c) top view.

7) After performing all the readings in relation to the x or y axis, rotate the sensor 180° and repeat the entire procedure;
8) Repeat all procedures in the position of the orthogonal groove of the guide tube to obtain displacement curves along the x and y axes;
9) Type "n" to end the program.

The digital readout response is converted to a tilt angle (α) via the sensor calibration equations (Equations 3 and 4), which consider the sensor offset parameters and sensitivity for the calculation of the offset value for the specific quota based on Equation 1.

During the cyclical routine of the Python program and with the help of the Pi Zero board, the data are transferred to the computer via cable. When all measurements for a given axis have been taken, the average probe displacement is calculated in relation to depth.

The accumulated average displacement is calculated from the sum of the average displacements at each elevation measured based on Equation 2. All accumulated readings are listed using an Excel spreadsheet and graphs are built per series of readings.

6. Methods

The probe was calibrated using a three-dimensional measuring table (coordinate measuring machine; SCIROCCO 100907 model TWPH10M; DEA) at the Department of Mechanical Engineering of PUC-PR (Pontifical Catholic University of Paraná), Brazil (Figure 11). This machine is used for the three-dimensional measurement of points with a linear optical transducer coupled to a mechanical arm that moves through pneumatic skates in three axes and is handled with a joystick. It has a measurement field of x = 1400 mm, y = 860 mm, and z = 660 mm, an approximate speed of 52 m/min (up to 65 m/min in fly function), and a measurement resolution of 2 µm.

As this equipment is not practically used for this purpose, an alternative calibration method was created. A calibration apparatus (Figure 11a) was built and fixed to the upper end of the probe, permitting rotation in one direction as a screw was rotated, generating a rotation angle. The rotation response was captured by the three-dimensional coordinates measured by the linear optical transducer for the generation of virtual sections. These sections were created from three points on the probe surface, which were used to generate the center of a partial circumference (Figure 11b). The generation of two sections resulted in the construction of a virtual cylinder whose generatrix inclination enabled the measurement of rotation angles in two directions (main and residual − in which slight equipment rotation generates a small error). These angles were compared with the digital output readings from the MEMS sensors (Figure 11c).

For validation, the experimental inclinometer probe was submitted to displacement reading tests performed through

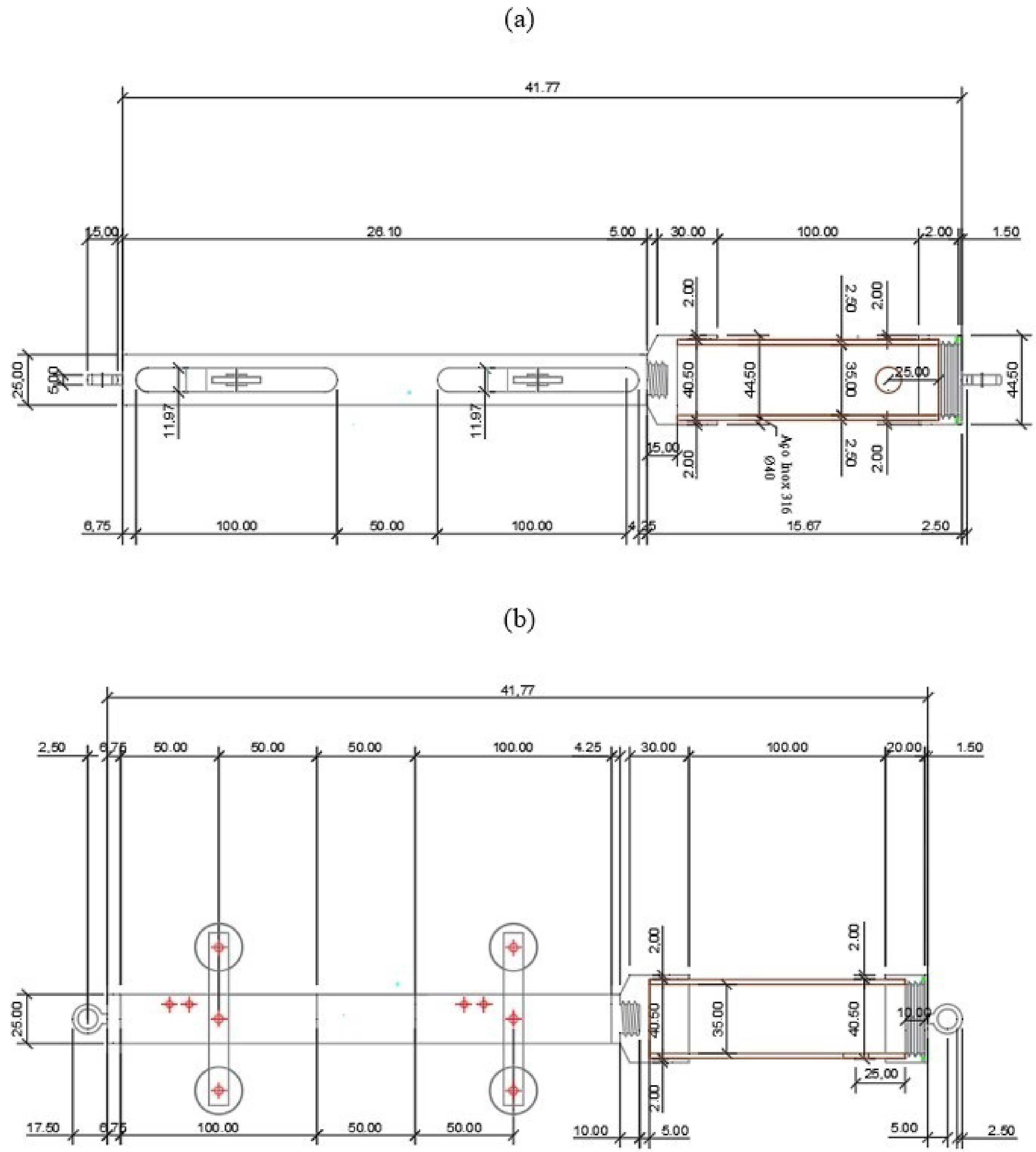

Figure 8. Geometric dimensions of the inclinometer probe (in millimeters): (a) A–A' section; (b) B–B' section.

an aluminum guide tube (φ_{ext} = 85 mm, length = 3 m) fixed to a metallic structure (Figure 12). To assess the sensitivity of the equipment, fictitious distortions were created at specific points using clamps (Figure 12a and 12b).

The probe used for comparison was the Digitilt Datamate II (DGSI; Figure 13a), a classic type of slope indicator with which readings are obtained via the digital responses of the sensor, converted from the axis distance using the sensor's calibration coefficient. Figure 13b shows the experimental measurement system with the inclinometer probe coupled to a notebook and the program file open.

The tests were performed between -0.5 and -2.5 m due to the restrictions of the commercial probe with regard to the 3 m-long guide tube; the probe has a length of approximately

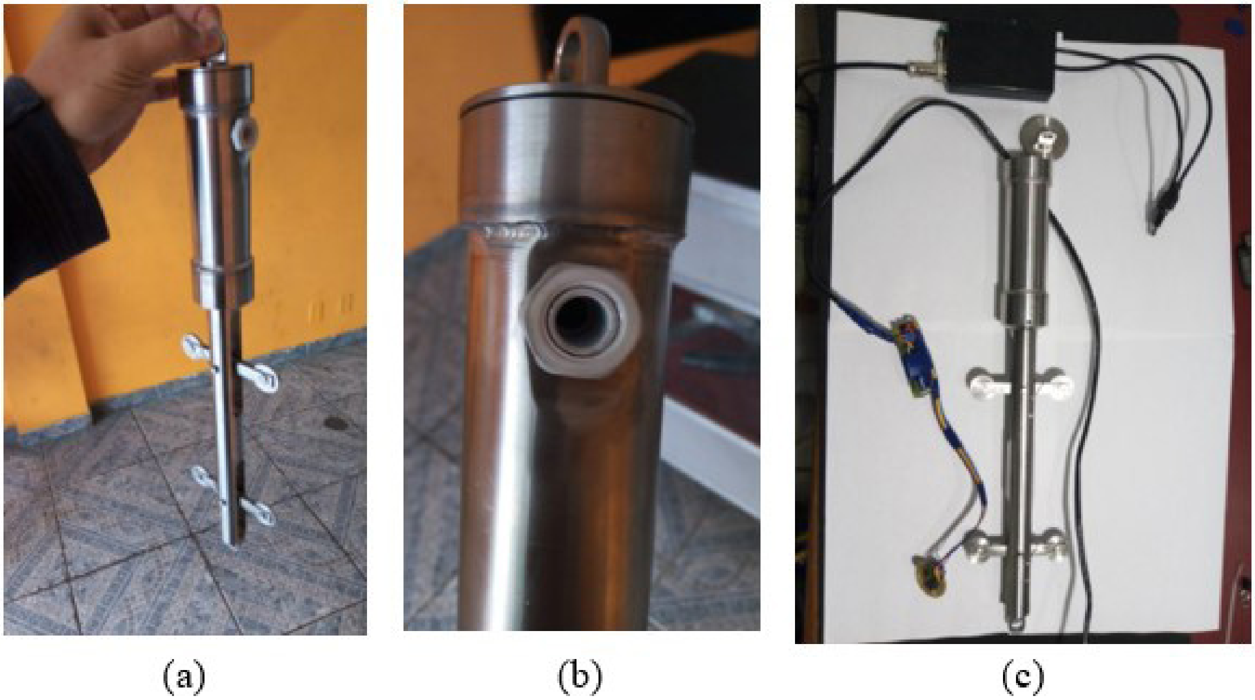

Figure 9. Inclinometer probe body: (a) welded machined parts; (b) detail of the cable gland for the passage of the power and reading cable: (c) the probe with the electronic circuit and USB adapter for notebook access.

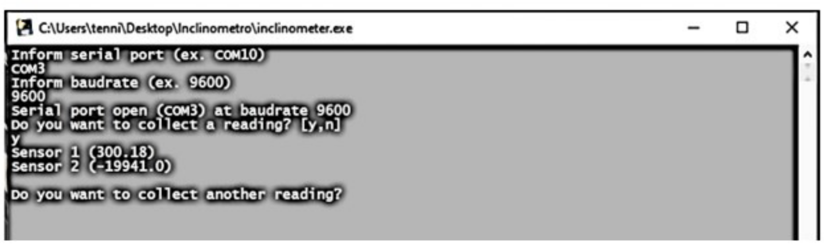

Figure 10. Python program commands to obtain readings.

60 cm and thus could not descend to the bottom of the tube for measurement, and it was impeded at the top due to the absence of an adequate centralizing CAP. The test followed the standard procedure for inclinometer-based measurement: horizontal displacement was measured with each probe in the 0º and 180º positions along the *x* and *y* axes (total = 4 measurements). The measurement procedure was not repeated because the magnitude of the horizontal displacement in both directions was known.

7. Results and discussion

Figure 14 shows the assembled electronic circuit for data reading and transfer. Figure 14a shows how the sensor was attached to the body of the inclinometer and Figure 14b shows the complete circuit with the MEMS sensor connection on the Raspberry Pi Zero® W board and its modules.

Figure 15 shows the inclinometer probe components in the final phase. Figure 15a shows the communication black box for the protection and Figure 15b shows the positioning of the MEMS sensors on the probe by means of labels. The stainless-steel reinforced signal-sending cable is marked every 15 cm with nylon clamps and accumulated length identifications to facilitate the depth readings (Figure 15c).

7.1 Inclinometer probe body

Probe calibration revealed an excellent linear relationship between the digital readings from sensor S1 and the angle (Figure 16). The offset value was –57.4231 and the sensitivity value was 6500.6001($R^2 = 1$).

For sensor S2, a non-linear response was observed at reading values close to 10° and the magnitude of the

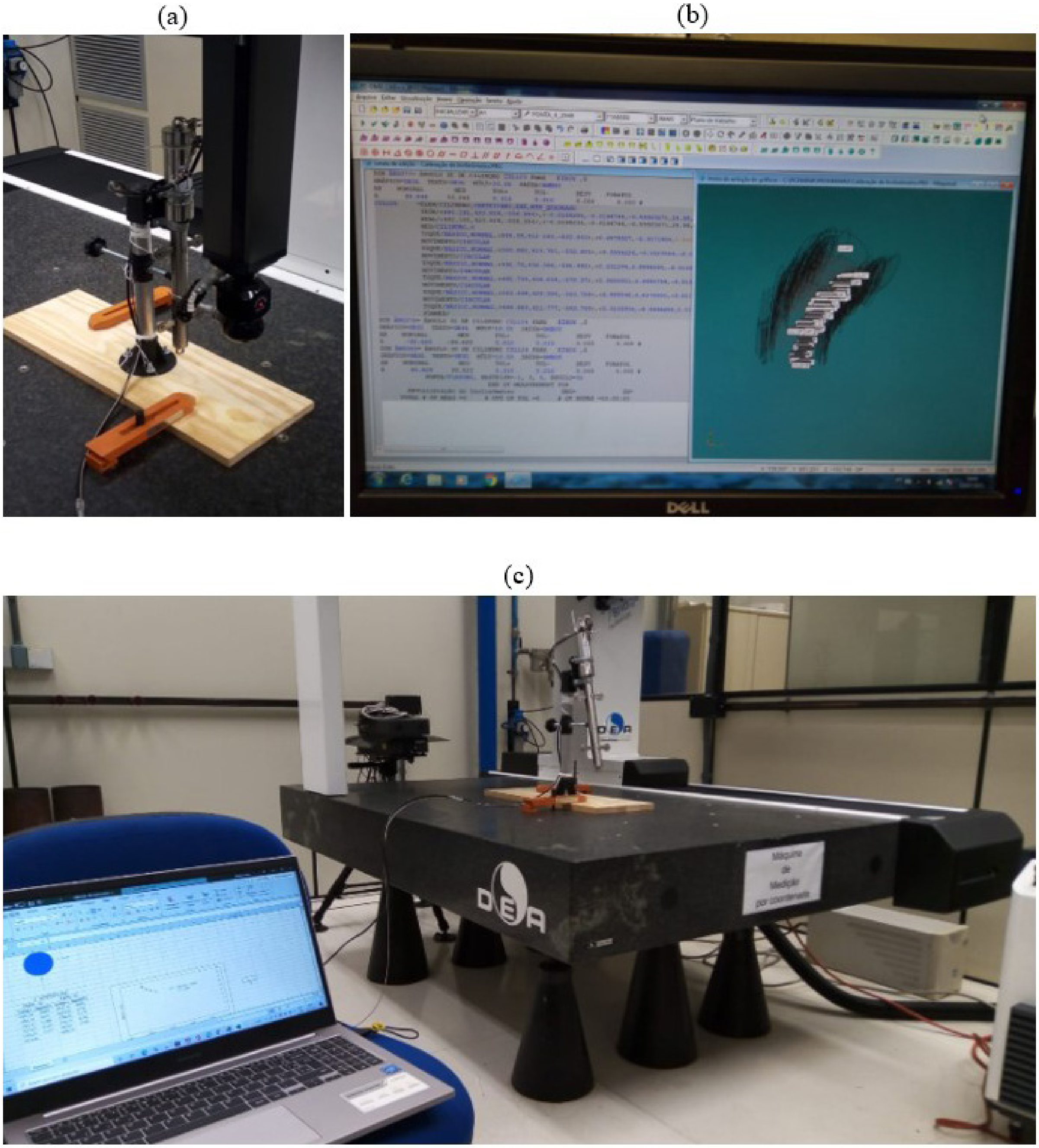

Figure 11. Inclinometer probe calibration: (a) measurement; (b) virtual cylinder development; (c) comparison of measurements with digital readings.

digital readings was greater than that for sensor S1 due to analog/digital output conversion. In the main reading direction, the measured angles and digital readings correlated excellently (R^2 = 0.985; Figure 17a). However, noise was observed in digital readings ranging from -7000 to 8600 (Figure 17b) when calibrating the S2 sensor. These digital values from the main direction represent significant rotation angles and consequently satisfactory horizontal displacement.

7.2 Comparison of commercial and experimental inclinometer probe performance

Figure 18 shows the measured horizontal displacements as functions of the measured depth for both probes. The displacement curves for the x axis are similar (Figure 18a), reflecting efficient and accurate performance of the experimental probe with <0.5 mm variation. In contrast, significant discrepancies were observed along the y axis (Figure 18b).

Figure 12. Guide tube used to validate the experimental probe: (a) distortion along the *y* axis; (b) distortion along the *x* axis; (c) introduction of the commercial probe into the guide tube.

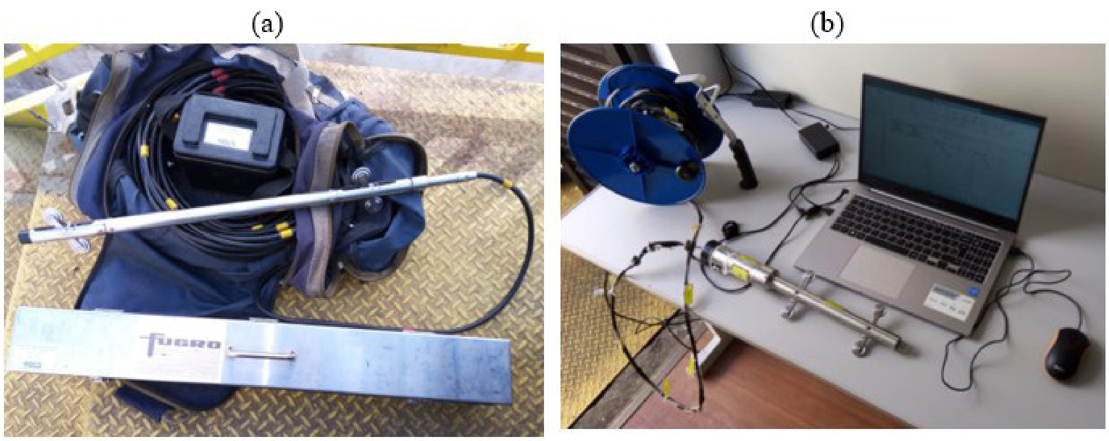

Figure 13. Inclinometer probes used: (a) Digitilt Datamate II; (b) experimental probe coupled to a notebook.

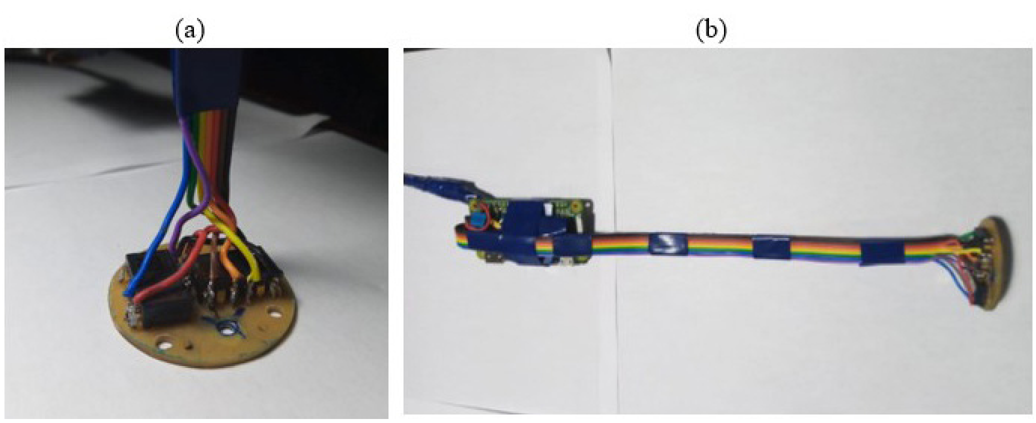

Figure 14. Construction of the inclinometer's electronic circuit: (a) the inclinometer installed on the base; (b) the reading electronic circuit.

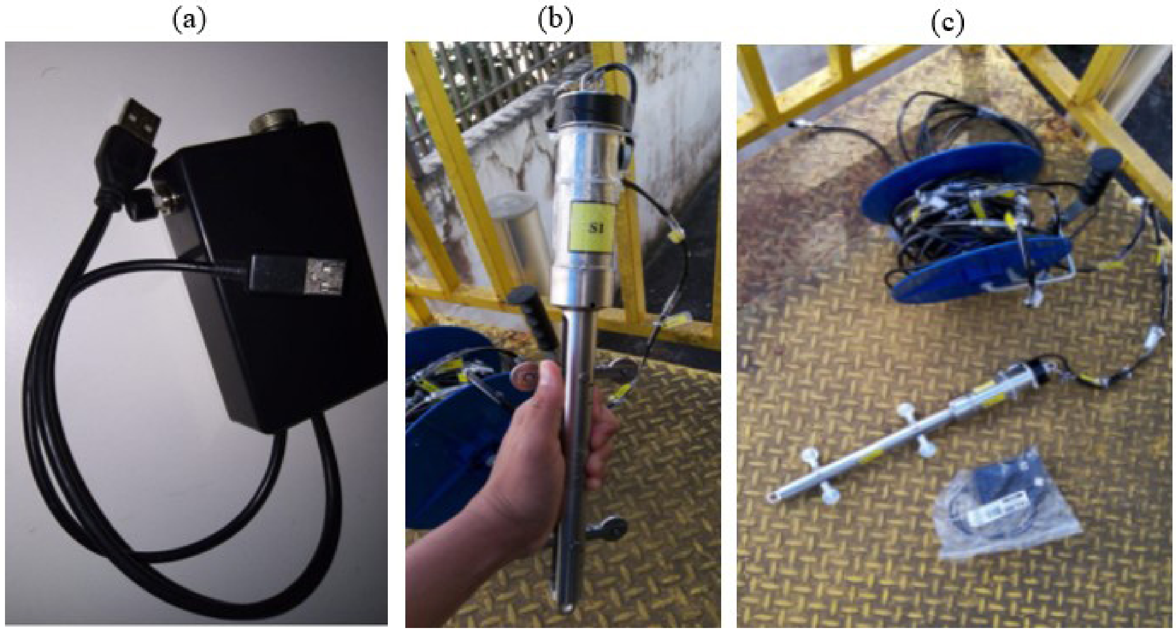

Figure 15. UFRGS inclinometer: (a) black box for communication; (b) inclinometer probe; (c) reading system components.

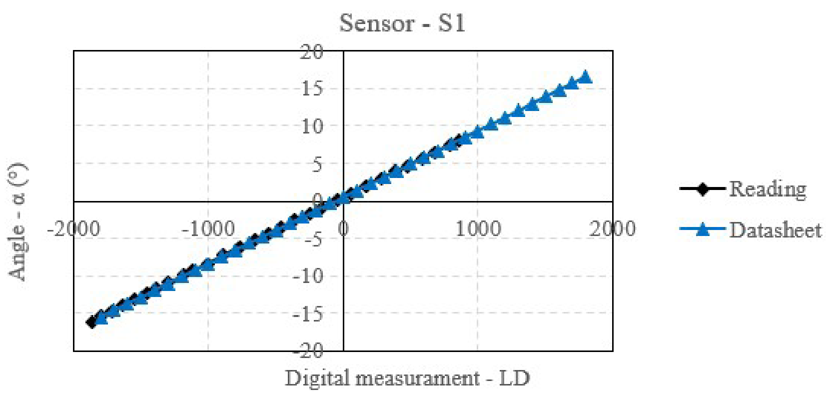

Figure 16. MEMS sensor S1 calibration.

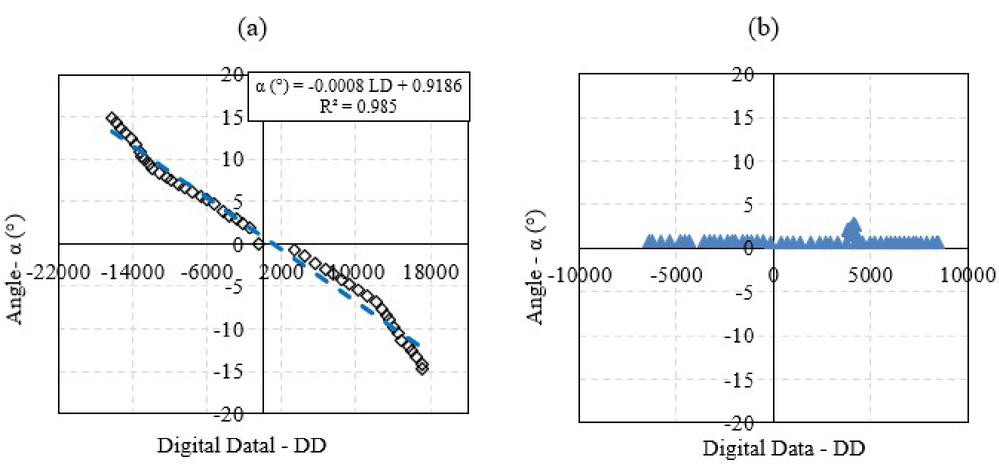

Figure 17. MEMS sensor S2 calibration: (a) principal direction; (b) direction perpendicular to the principal.

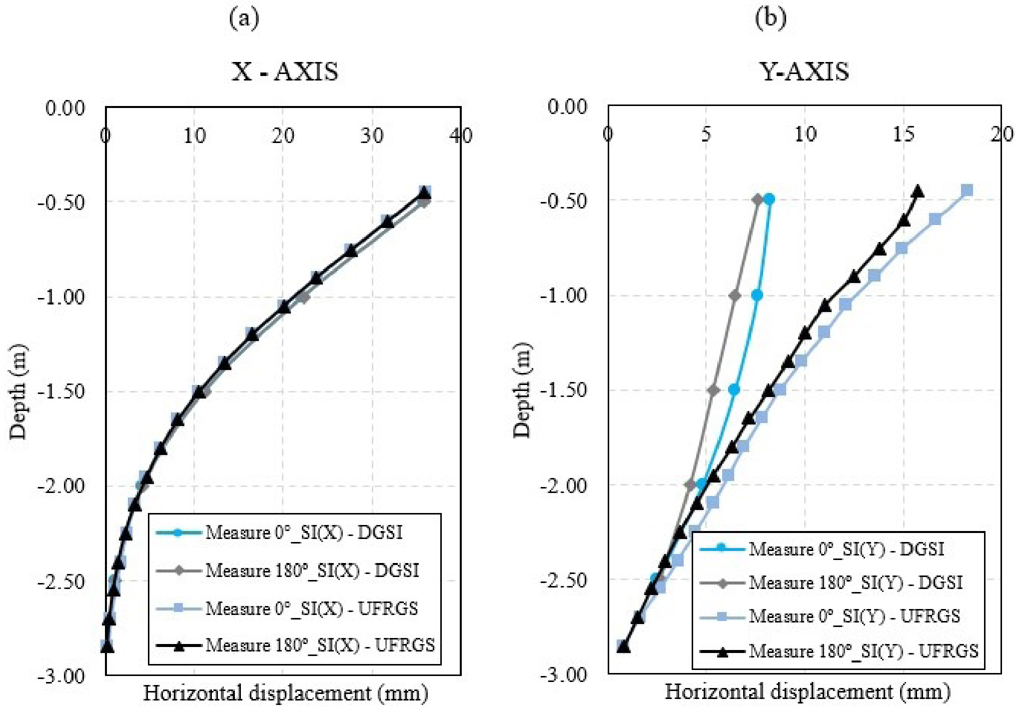

Figure 18. Comparison of results from the Digitilt Datamate II commercial probe and the UFRGS experimental inclinometer: (a) *x* axis; (b) *y* axis.

The greatest displacement measured by the commercial probe was approximately 8 mm, whereas that measured by the experimental probe was 17 mm. Considering that sensor S1 was used to obtain measurements along both axes, the low value generated by the commercial probe was considered to be inaccurate.

8. Conclusions

This work demonstrated that a low-cost probe for the measurement of horizontal displacement comparable to commercial probes can be developed with simple and accessible technology, such as precise MEMS sensors, microprocessor boards, and Python programming. This low-cost probe can feasibly be used for the monitoring of geotechnical structures (e.g., dams, reservoirs, slopes, mountains, and landfills) when management entities (e.g., mining companies, commodity exploration companies, and public institutions) do not have sufficient financial resources to implement extensive and safe site monitoring programs. Based on the results obtained, the following conclusions can be made about the inclinometer probe:

a) The probe's measurement of displacement along the *x* axis was consistent with that of a commercial probe This is an indication that the probe has been properly calibrated and valid;
b) The three-dimensional probe calibration method used in this study was an applicable and accurate alternative. Through the comparison study between the experimental probe and the commercial probe it was observed that there were few differences in the horizontal displacement graph along the depth.

Acknowledgements

The authors would like to express their gratitude to the Brazilian National Council for Scientific and Technological Development (CNPq) – project 309455/2020-0 and Brazilian Coordination for the Improvement of Higher Education Personnel (CAPES).

Declaration of interest

The authors have no conflict of interest, financial or otherwise, to declare. All authors have read and approved the contents of the paper.

Authors' contributions

Tennison Freire de Souza Junior: Conceptualization, Data curation, Methodology, Visualization, Validation, Writing – original draft (in Portuguese). José Lucas Silva Borges: Conceptualization, Data curation, Software (phyton algorithm), Methodology, Investigation. Cezar Falavigna Silva: Formal Analysis, Writing – original draft (in Portuguese), Translation to English – original draft. Writing – review &

editing. Karla Salvagni Heineck: Formal Analysis, Funding acquisition, Supervision, Resources, Writing – review & editing.

The authors above kindly granted permission to use parts of their publications in this paper.

Data availability

All data produced or examined in the course of the current study are included in this article.

List of symbols and abbreviations

$tilt_n$:	the amount of tilt angle in degrees
ARM:	Acorn Risc Machine
COM:	Communication Port
CPU:	Central Processing Unit
HAT:	Hardware Attached on Top
HDMI:	High-Definition Multimedia Interface
K_r:	pile stiffness, as a structural piece
L:	distance between inclinometer wheels
MEMS:	Micro-Electro-Mechanical Systems
NTSC:	National Television System(s) Committee
Q_{ffset}:	device output in the 0° tilt position
OTG:	On the go
PAL:	Phase Alternating Line
PUC-PR:	Pontifical Catholic University of Paraná
RAM:	Random Access Memory
UART:	Universal Asynchronous Receiver-Transmitter
USB:	Universal Serial Bus
$V_{D,out}$:	output voltage of differential amplifier
V_{out}:	differential amplifier output
$V_{out_{tilt1}}$:	measured output in tilt 1 position
$V_{out_{tilt2}}$:	measured output in tilt 2 position
δ_{DH}:	displacement generated by the guide tube at a given depth
δ_{DHT}:	total horizontal displacement (from top to fixed end)
φext:	external diameter

References

Adafruit. (2019). *Introducing the Raspberry Pi Zero.* Retrieved in July 9, 2019, from https://learn.adafruit.com/introducing-the-raspberry-pi-zero/a-tour-of-the-pi-zero

ASTM A479. (2007). *Standard specification for stainless steel bars and shapes for use in boilers and other pressure vessels.* ASTM International, West Conshohocken, PA.

Bartholomew, C.L., Murray, B.C., & Goins, D.L. (1987). *Embankment instrumentation manual*. Washington, DC: Bureau of Reclamation.

Bo, M.W., & Barrett, J. (2023). *Geotechnical instrumentation and applications*. Cham: Springer. http://doi.org/10.1007/978-3-031-34275-2.

Carbó, H.M. (2008). *Aços inoxidáveis: aplicações e especificações.* ArcelorMittal (in Portuguese). Retrieved in July 7, 2019, from https://perma.cc/79NE-6RRX

Coimbra, L., Salgado, F., & Meixedo, J.P. (2023). Slope inclinometers: qualitative evaluation of probe inclinometer data: an update. In *Proceedings of the 1st Conference on Georesources, Geomaterials, Geotechnologies and Geoenvironment* (pp. 137-140), Porto. Cham: Springer. http://doi.org/10.1007/978-3-031-25986-9_23.

Covassi, P.A., Kunz, R., Nadal, D., Bossio, C., & Covassi, M.E. (2018). Vigas clinométricas: tecnologia y aplicaciones. In *24º Congreso Argentino de Mecánica de Suelos e Enginieria Geotécnica* (pp. 1-18), Salta. SAIG (in Spanish).

Dunnicliff, J. (1988). *Geotechnical instrumentation for monitoring field performance*. New York: John Wiley & Sons.

Fernandes, M.M. (2011). *Mecânica dos solos: introdução à engenharia geotécnica* (Vol. 2). São Paulo: Oficina de Textos (in Portuguese).

Formoso, M.T. (1999). *Desenvolvimento de um inclinômetro para monitorar o comportamento de taludes instáveis de solos* [Master's dissertation, Federal University of Rio Grande do Sul]. Federal University of Rio Grande do Sul's repository (in Portuguese). Retrieved in April 11, 2019, from http://hdl.handle.net/10183/119377

Freddi, F., Mingazzi, L., Pozzi, E., & Aresi, N. (2023). Laboratory assessment of an in-place inclinometer chain for structural and geotechnical monitoring. *Sensors*, 23(20), 8379. http://doi.org/10.3390/s23208379.

Green, G.E., & Mikkelsen, P.E. (1988). Deformation measurements with inclinometers. *Transportation Research Record: Journal of the Transportation Research Board*, (1169), 1-15.

Hanna, T.H. (1985). *Field instrumentation in geotechnical engineering*. Rockport: Trans Tech Publications.

Hunt, R.E. (2005). *Geotechnical engineering investigation handbook* (2nd ed., 1088 p.). Boca Raton: Taylor & Francis Group. http://doi.org/10.1201/9781420039153.

Machan, G., & Bennett, V.G. (2008). *Use of inclinometers for geotechnical instrumentation on transportation projects: state of practice* (Transportation Research Circular, No. E-C129). Washington, DC: Transportation Research Board.

Maxim. (2014). *Low-power, slew-rate-limited RS-485/RS-422 transceivers.* Retrieved in July 1, 2023, from https://www.analog.com/en/products/max485.html

Mikkelsen, P.E. (2002). Cement–bentonite grout backfill for borehole instruments. *Geotechnical News*, 20(4), 38-42.

Mikkelsen, P.E. (2003). Advances in inclinometer data analysis. In *Proceedings of the 6th International Symposium on Field Measurements in Geomechanics* (pp. 1-13), Oslo. CRC Press.

Murata. (2019). *SCA103T-D04-1.* Retrieved in April 11, 2019, from https://perma.cc/WV4K-ECTN

Penz, S.R. (2013). *Desenvolvimento de um inclinômetro com tecnologia MEMS aplicado ao monitoramento de* *obras geotécnicas* [Master's dissertation, Passo Fundo University]. Passo Fundo University's repository (in Portuguese). Retrieved in April 11, 2019, from http://tede.upf.br:8080/jspui/handle/tede/299

Silveira, J.F.A. (2006). *Instrumentação e segurança de barragens de terra e enrocamento*. São Paulo: Oficina de Textos (in Portuguese).

Souza, H.G., Ehrlich, M., Dieguez, C.A., & Salviano, A.L.S. (2016). Aferição da performance de sondas inclinométricas através de sistema de calibração e resultados de campo. In *Anais do Congresso Brasileiro de Mecânica dos Solos*, Belo Horizonte (pp. 1-6). ABMS.

Stark, T.D., & Choi, H. (2008). Slopes inclinometers for landslides. *Landslides*, 5(3), 339-350. http://doi.org/10.1007/s10346-008-0126-3.

Wilson, S.D. (1962) The use of slope measuring devices to determine movements in earth masses. In *Proceedings of the Symposium on field testing of soils* (pp. 187-198), New York. West Conshohocken, PA: ASTM. http://doi.org/10.1520/STP47040S.